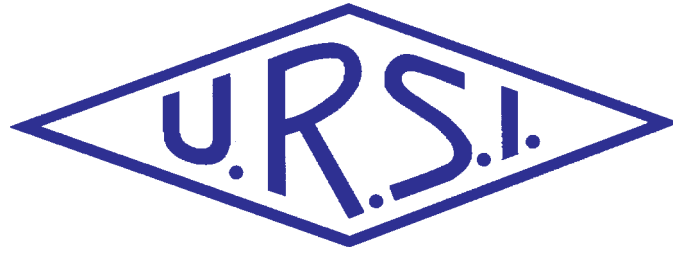


Radio Science Bulletin

ISSN 1024-4530

INTERNATIONAL
UNION OF
RADIO SCIENCE

UNION
RADIO-SCIENTIFIQUE
INTERNATIONALE



No 345
June 2013

URSI, c/o Ghent University (INTEC)
St.-Pietersnieuwstraat 41, B-9000 Gent (Belgium)

Contents

Editorial	3
URSI GASS 2014	5
Awards for Young Scientists - Conditions	6
Introduction to the Special Section on the Role of Radio Science in Disaster management	7
Topology Modeling and Network Partitioning : An Application to Forest-Fire Fighting	8
Causal Probabilistic Modeling with Bayesian Networks to Combat the Risk of Piracy Against Offshore Oil Platforms	21
Application of the Extended Ground Truth Concept for Risk Anticipation Concerning Ecosystems	35
Two-Tier Femto-Macro Wireless Networks : Technical Issues and Future Trends	51
An Analog of Surface Tamn States in Periodic Structures on the Base of Microstrip Waveguides	64
Book Reviews for Radioscientists	73
Conferences	76
News from the URSI Community	81
Call for Papers	89
Information for authors	92

Front cover: (top) The Faucon Noir unmanned aerial system in flight, with one its mapping payloads. (bottom) A mosaic created with the oblique images taken by the aerial system. See the paper by Antoine Gademer, Laurent Beaudoin, Loïca Avanthey, and J. P. Rudant in the "Special Section on the Role of Radio Science in Disaster Management."

EDITOR-IN-CHIEF
URSI Secretary General
Paul Lagasse
Dept. of Information Technology
Ghent University
St. Pietersnieuwstraat 41
B-9000 Gent
Belgium
Tel.: (32) 9-264 33 20
Fax : (32) 9-264 42 88
E-mail: ursi@intec.ugent.be

EDITORIAL ADVISORY BOARD
Phil Wilkinson
(URSI President)
W. Ross Stone

PRODUCTION EDITORS
Inge Heleu
Inge Lievens

SENIOR ASSOCIATE EDITORS
O. Santolik
A. Pellinen-Wannberg

ASSOCIATE EDITOR FOR ABSTRACTS
P. Watson

ASSOCIATE EDITOR FOR BOOK REVIEWS
K. Schlegel

EDITOR
W. Ross Stone
840 Armada Terrace
San Diego, CA92106
USA
Tel: +1 (619) 222-1915
Fax: +1 (619) 222-1606
E-mail: r.stone@ieee.org

ASSOCIATE EDITORS

P. Banerjee & Y. Koyama (Com. A)	S. Paloscia (Com. F)
A. Sihvola (Com. B)	I. Stanislawska (Com. G)
S. Salous (Com. C)	M.M. Oppenheim (Com. H)
P-N Favennec (Com. D)	J. Baars (Com. J)
D. Giri (Com. E)	E. Topsakal (Com. K)

For information, please contact :

The URSI Secretariat
c/o Ghent University (INTEC)
Sint-Pietersnieuwstraat 41, B-9000 Gent, Belgium
Tel.: (32) 9-264 33 20, Fax: (32) 9-264 42 88
E-mail: info@ursi.org
<http://www.ursi.org>

The International Union of Radio Science (URSI) is a foundation Union (1919) of the International Council of Scientific Unions as direct and immediate successor of the Commission Internationale de Télégraphie Sans Fil which dates from 1913.

Unless marked otherwise, all material in this issue is under copyright © 2013 by Radio Science Press, Belgium, acting as agent and trustee for the International Union of Radio Science (URSI). All rights reserved. Radio science researchers and instructors are permitted to copy, for non-commercial use without fee and with credit to the source, material covered by such (URSI) copyright. Permission to use author-copyrighted material must be obtained from the authors concerned.

The articles published in the Radio Science Bulletin reflect the authors' opinions and are published as presented. Their inclusion in this publication does not necessarily constitute endorsement by the publisher.

Neither URSI, nor Radio Science Press, nor its contributors accept liability for errors or consequential damages.

An Analog of Surface Tamm States in Periodic Structures on the Base of Microstrip Waveguides



D.P. Belozorov
A.A. Girich
S.I. Tarapov

Abstract

The Tamm state concept was formulated for periodic systems consisting of microstrip elements by analogy with the well-known Tamm state in photonic crystals. The unit cell, which determines the period of our microstrip system, consists of four elements: two segments with lengths L_1 and L_2 , and two connections (1,2) and (2,1). The total period of the structure is equal to $L = L_1 + L_2$. The transfer matrix for the unit cell is written. The Bloch equation for the infinite system is formulated from the conditions of periodicity. The solutions of the Bloch equation determine the Bloch wave vector and the spectral structure of our infinite system. The numerical calculations of an important model system were performed. The model system consisted of two periodic subsystems (eight elements in either of the two), with different parameters of periodicity. The analog of the Tamm state was observed as a crowding of electromagnetic waves propagating through the system at the transition between two subsystems. The concentration of electromagnetic-wave energy takes place at the border point of one-dimensional subsystems. A corresponding transparency peak (a Tamm peak) appears in the coinciding forbidden frequency bands of two subsystems.

1. Special Properties of a Quadripole (Four-Pole) Medium

Currently, the study of bounded periodic structures (photonic crystals) and the condition for surface states to appear at the interface separating these structures had attracted the unceasing interest of researchers. The topic we are going to discuss now is connected with the well-known surface Tamm states appearing at the boundary of the bounded periodic structures: solid state lattices and

photonic crystals [1, 2]. An important feature of such surface Tamm states is the absence of tangential components of the Bloch wave vector at the interface, which means that any physical transfer of energy along the boundary is absent.

A narrow transparency peak (the Tamm peak) appears in the spectrum bandgap of a bounded periodic structure. The position of the peak in the frequency bandgap depends on the parameters characterizing the whole system. This allows us to use this system in a variety of practical applications: for example, such as a controlled filter of electromagnetic radiation. The theoretical and experimental study of Tamm states in one-dimensional periodic crystals was discussed in a number of papers (see, e.g., [3, 4, 5, 6]).

The purpose of this paper is to study the analog of Tamm states for special bounded periodic structures consisting of microstrip elements, the elements of which are now widely used in various microwave applications. In particular, note the usage of microstrip photonic crystals for measurements of the permittivity of fluid substances [7].

We shall not dwell on the strengths and weaknesses of the existing theory of microstrip circuits [8]. However, it should be noted that because of complex mathematics, their detailed theory is far behind its practical applications, and is still far from being complete. However, there are a number of approximate formulas for quite accurately describing these waveguide systems, depending on their design features and the microwave frequency range [9-16].

If we are dealing with an infinite periodic structure, i.e., a symmetrical structure with respect to periodic translations by vector \mathbf{L} , all fields at points separated by a vector translation \mathbf{L} are known to be connected by the relationships

D. P. Belozorov is with the Institute for Theoretical Physics, NSC "Kharkov Institute of Physics & Technology" NAS of Ukraine, Kharkov, Ukraine, Akademicheskaja St., Kharkov 61108, Ukraine; E-mail: belodi36@gmail.com. A. A. Girich and S. I. Tarapov are with the Institute of Radiophysics and Electronics NAS of Ukraine, 12 Ac. Proskura st., Kharkov, 61085, Ukraine; Tel: +38057-720-3463; Fax: +38057-315-2105; E-mail: girich82@mail.ru; tarapov@ire.kharkov.ua.

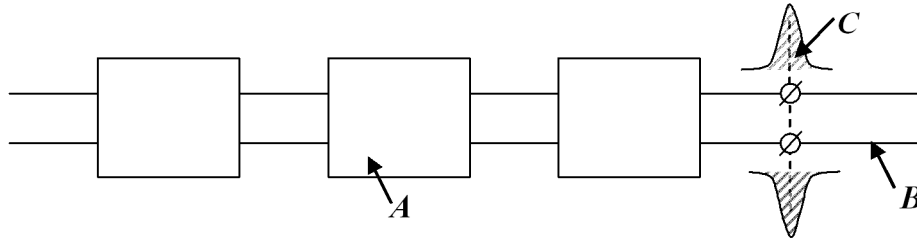


Figure 1. The schematic for observation of the Tamm states. A is the chain of four-poles (Medium 1), B is the line with strong attenuation or the similar subsystem with different parameters (Medium 2), and C is the analog of the Tamm states. C shows the “concentration” of the electromagnetic energy near the interface of four-pole systems A and B.

$$\mathbf{E}(x, y, z + L) \exp(ik_B L) = \mathbf{E}(x, y, z), \quad (1)$$

$$\hat{\mathbf{T}} = \prod_{i=1}^k \hat{\mathbf{T}}_i, \quad (2)$$

where k is the number of four-poles in the chain.

$$\mathbf{H}(x, y, z + L) \exp(ik_B L) = \mathbf{H}(x, y, z).$$

For electromagnetic waves in one-dimensional periodic systems, the quantity k_B , called the Bloch vector, is scalar. The conditions of Equations (1) are known as the Floquet condition (Floquet theorem) for the case of one-dimensional periodicity, and the Bloch condition (Bloch theorem) when the system is periodic in two dimensions or three dimensions. The proof of the statement in Equation (1) reduces to the known fact from linear algebra that at least one solution, \mathbf{U} , exists for any square matrix, $\hat{\mathbf{A}}$, which satisfies the equation $\hat{\mathbf{A}}\mathbf{U} = \mu\mathbf{U}$ (see, e.g., [9]).

Below, we present our system as a chain of two-lines consisting of micro-strips (see Figure 1). We use the well-known formalisms of a normalized wave-transmission matrix, $\hat{\mathbf{T}}$, a normalized wave-scattering matrix, $\hat{\mathbf{S}}$, and the normalized classical transmission matrix, $\hat{\mathbf{A}}$, for description of the chain. All of these matrices are related to each other, so elements of one matrix can be expressed in terms of another (for details about the properties of these matrices, see [10-12]). Note here the important property of the transmission matrix of the system, namely, that the transmission matrix of a cascade (chain) of four-poles is the product of the transmission matrices for individual four-poles:

Considering the wave processes in a medium that represents a periodic sequence of identical four-poles, we single out two variants of the medium. The first variant is the sequence of elementary cells unbounded in both directions (Medium 1). The second variant is the same sequence of cells bounded from one side. In the latter case, the sequence of four-poles is usually supposed to be bounded with a Medium 2, where the wave process becomes heavily attenuated. Tamm states are known to be surface states appearing at the interfaces of adjacent different photonic crystals. Here, we deal with one-dimensional systems of micro-strips, so at the border point of two different subsystems, we shall speak only about the analog of the Tamm states. [1, 3, 4].

The process at the medium of the four-poles in approximation of the wave-transmission matrix is a voltage wave connected with a conditional wave process that takes place in a long line, equivalent to given system of four-poles. Here, properties of an individual four-pole are determined by its wave-transmission matrix, $\hat{\mathbf{T}} = (T_{ik})$ [10, 11], and (Figure 2)

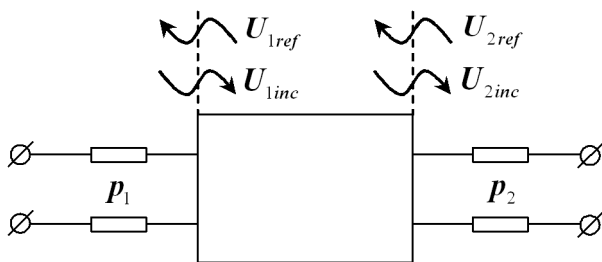


Figure 2. The circuit of a four-pole.

$$U_{inc}^n = T_{11}U_{2inc}^n + T_{12}U_{2ref}^n,$$

$$U_{1ref}^n = T_{21}U_{2inc}^n + T_{22}U_{2ref}^n, \quad (3)$$

$$U_{1inc} = t_{11}U_{2inc} + t_{12}U_{2ref},$$

$$U_{1ref} = t_{21}U_{2inc} + t_{22}U_{2ref},$$

$$(T_{ik}) = \sqrt{\rho_1 \rho_2^{-1}} (t_{ik}).$$

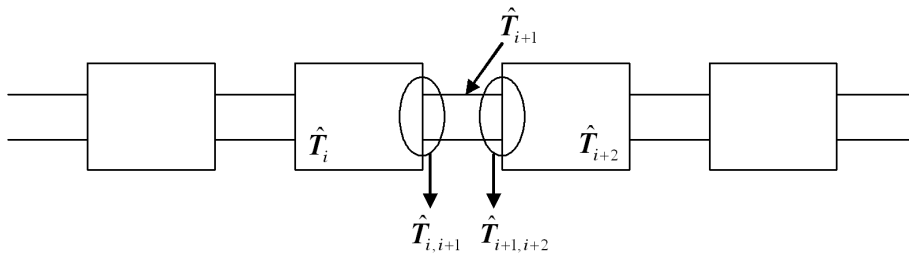


Figure 3a. An infinite periodic chain of four-poles.

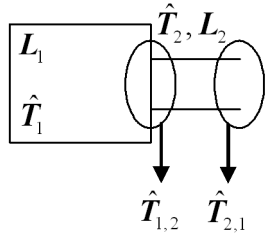


Figure 3b. The unit cell of the periodic structure of Figure 3a.

U_{1inc}^n , U_{1ref}^n , U_{2inc}^n , and U_{2ref}^n are the normalized incident and reflected voltage waves in the transmission lines at the input and output of the four-pole:

$$U_{1inc,ref}^n \sqrt{\rho_1} = U_{1inc,ref}^n,$$

$$U_{2inc,ref}^n \sqrt{\rho_2} = U_{2inc,ref}^n.$$

Here, U_{1inc} , U_{2inc} , U_{1ref} , and U_{2ref} are the complex amplitudes of the incident and reflected waves, and ρ_1 and ρ_2 are the wave impedances of the input and output lines.

Note that in addition to a normalized wave in terms of the transmission matrix, as we shall see below an important physical meaning also has a normalized wave in terms of the scattering matrix $\hat{S} = (S_{ik})$. The elements of the scattering matrix are expressed in terms of elements of the matrix \hat{T} in the following way:

$$U_{1ref}^n = S_{11}U_{1inc}^n + S_{12}U_{2ref}^n,$$

$$U_{1inc}^n = S_{21}U_{1inc}^n + S_{22}U_{2ref}^n, \quad (4)$$

$$\hat{S} = \begin{pmatrix} S_{11} & S_{12} \\ S_{21} & S_{22} \end{pmatrix} = \begin{pmatrix} \frac{T_{21}}{T_{11}} & \frac{|T|}{T_{11}} \\ \frac{1}{T_{11}} & \frac{-T_{12}}{T_{11}} \end{pmatrix}.$$

Here, $|T| = \det \hat{T}$.

One can mention here the physical meaning of the elements of both matrices \hat{T} and \hat{S} , which are associated with a certain “characteristic” mode in the system of four-poles. In the wave theory, the role of such a “typical” mode is as a mode with zero parameter Γ_N , the reflection coefficient from a load of the output line:

$$\Gamma_N = \frac{U_{2ref}^n}{U_{2inc}^n}. \quad (5)$$

In other words, $U_{2ref}^n = 0$. In this case,

$$T_{11} = \frac{U_{1inc}^n}{U_{2inc}^n},$$

$$T_{21} = \frac{U_{1ref}^n}{U_{2inc}^n}, \quad (6)$$

$$S_{11} = \frac{U_{1ref}^n}{U_{1inc}^n},$$

$$S_{21} = \frac{U_{2inc}^n}{U_{1inc}^n}.$$

The elements of the matrices T_{11} , S_{21} , and S_{11} determine the properties of a four-pole loaded with a matched line at the definite forward direction of wave propagation (left to right). In particular, T_{11} determines the ratio of the normalized voltages in this mode, and is called the transmission coefficient. $S_{21} = T_{11}^{-1}$, and has an individual name, the “transmittance.” $D = |T_{11}|^{-2}$ is used as the microwave power-transmission coefficient [7]. S_{11} is the reflection coefficient in the input line with matched output line. The microwave power reflection coefficient from the microstrip photonic structure is defined as $R = |S_{11}|^2$ [7].

2. Bloch Equation

We now consider an infinite periodic chain of identical four-poles (microstrip waveguides), and define the equation for the Bloch wave vector in such a structure. The transmission matrix for the elementary cell of the periodic structure, which consists of a complex four-pole (see Figure 3b), is the product of the wave-transmission matrices of four-poles constituting the elementary cell, and respectively including the following elements: the i th segment, a direct connection to the i th and $(i+1)$ segments, the $(i+1)$ segment, and the direct connection of the $(i+1)$ and $(i+2)$ segments of the microwave transmission line. The infinite periodic chain of four-poles and its unit cell are sketched in Figures 3a and 3b.

We see that the unit cell that determines the period of our structure consists of segments with lengths L_1 and L_2 and of two connections, (1,2) and (2,1). The total period of the structure is therefore equal to $L = L_1 + L_2$.

Using the wave-transmission matrices for the elements of the structure without considering attenuation [7],

$$\hat{T}_S = \begin{bmatrix} \exp(ik_S L_S) & 0 \\ 0 & \exp(-ik_S L_S) \end{bmatrix},$$

$$\hat{T}_{S,S+1} = \begin{pmatrix} \frac{r_{S,S+1} + 1}{2\sqrt{r_{S,S+1}}} & \frac{r_{S,S+1} - 1}{2\sqrt{r_{S,S+1}}} \\ \frac{r_{S,S+1} - 1}{2\sqrt{r_{S,S+1}}} & \frac{r_{S,S+1} + 1}{2\sqrt{r_{S,S+1}}} \end{pmatrix}, \quad (7)$$

$$r_{S,S+1} = r_{S+1,S}^{-1} = \frac{\rho_{S+1}}{\rho_S}, \quad (s=1,2).$$

We obtain the following expression for the transmission-wave matrix of the unit cell:

$$\hat{\mathbf{T}}_{EC} = \hat{\mathbf{T}}_1 \hat{\mathbf{T}}_{1,2} \hat{\mathbf{T}}_2 \hat{\mathbf{T}}_{2,1}, \quad (8)$$

$$\hat{\mathbf{T}}_{EC} = \begin{pmatrix} T_{11}^{EC} & T_{12}^{EC} \\ T_{21}^{EC} & T_{22}^{EC} \end{pmatrix} \quad (9)$$

$$\det \hat{\mathbf{T}}_{EC} = T_{11}^{EC} T_{22}^{EC} - T_{12}^{EC} T_{21}^{EC} = 1$$

(so the transmission matrix is unimodular). The elements of the matrix $\hat{\mathbf{T}}_{EC}$ are equal to

$$T_{11}^{EC} = 4^{-1} \left(2 + r_{1,2} + r_{1,2}^{-1} \right) \exp(ik_1 L_1 + ik_2 L_2) \\ + 4^{-1} \left(2 - r_{1,2} - r_{1,2}^{-1} \right) \exp(ik_1 L_1 - ik_2 L_2),$$

$$T_{22}^{EC} = 4^{-1} \left(2 + r_{1,2} + r_{1,2}^{-1} \right) \exp(-ik_1 L_1 - ik_2 L_2) \\ + 4^{-1} \left(2 - r_{1,2} - r_{1,2}^{-1} \right) \exp(-ik_1 L_1 + ik_2 L_2), \quad (10)$$

$$T_{12}^{EC} = 4^{-1} \left(r_{1,2} - r_{1,2}^{-1} \right) \exp(ik_1 L_1 - ik_2 L_2) \\ - 4^{-1} \left(r_{1,2} - r_{1,2}^{-1} \right) \exp(ik_1 L_1 + ik_2 L_2),$$

$$T_{21}^{EC} = 4^{-1} \left(r_{1,2} - r_{1,2}^{-1} \right) \exp(-ik_1 L_1 + ik_2 L_2) \\ - 4^{-1} \left(r_{1,2} - r_{1,2}^{-1} \right) \exp(-ik_1 L_1 - ik_2 L_2).$$

We note that $(T_{11}^{EC})^* = T_{22}^{EC}$ and $(T_{12}^{EC})^* = T_{21}^{EC}$, as well as $|T_{11}^{EC}|^2 = 1 + |T_{21}^{EC}|^2$, so the wave matrix is a matrix of a reversible reactive four-pole [12].

The quantities ρ_S and k_S ($s=1,2$) entering Equations (7) and (10) are related to characteristics of structural elements (W_S is the width of the strip wire, h_S is the thickness of the microstrip-line substrate, and ϵ_S is the permittivity of the substrate). The wave resistance of the microstrip line according to [12, 14, 16] is therefore equal to

$$\rho_S = \frac{377 h_S}{\sqrt{\epsilon_S} W_S \left[1 + 1.735 \epsilon_S^{-0.0724} \left(\frac{W_S}{h_S} \right)^{-0.836} \right]} \quad (11)$$

where $k_S = 2\pi\Lambda_S^{-1}$.

The wavelength of the electromagnetic wave, Λ_S at the s th section of the microstrip line is defined by the known expression [7, 14, 16]

$$\Lambda_S = \begin{cases} \frac{\lambda}{\sqrt{\epsilon_S}} \sqrt{\frac{\epsilon_S}{1 + 0.63(\epsilon_S - 1) \left(\frac{W_S}{h_S} \right)^{0.1255}}} & \text{for } \frac{W_S}{h_S} \geq 0.6 \\ \frac{\lambda}{\sqrt{\epsilon_S}} \sqrt{\frac{\epsilon_S}{1 + 0.6(\epsilon_S - 1) \left(\frac{W_S}{h_S} \right)^{0.0297}}} & \text{for } \frac{W_S}{h_S} < 0.6 \end{cases} \quad (12)$$

where λ is the wavelength in vacuum. The formulas in Equation (12) give dispersion relations for electromagnetic waves in the s th section of the microstrip line.

In what follows, we restrict our attention to the traveling-wave regime, which corresponds to the absence of the reflected wave in the system. The normalized classical transmission matrix relates currents and voltages on both sides of the four-pole [11], i.e.,

$$U_1^n = A_{11}U_1^n + A_{12}I_2^n, \quad (13)$$

$$I_1^n = A_{21}U_2^n + A_{22}I_2^n,$$

$$\begin{pmatrix} U_1^n \\ I_1^n \end{pmatrix} = \hat{A} \begin{pmatrix} U_2^n \\ I_2^n \end{pmatrix},$$

where

$$U_l^n = U_{linc}^n + U_{lref}^n, \quad I_l^n = U_{linc}^n - U_{lref}^n, \quad (l=1,2).$$

Under the traveling-wave conditions, the voltage and current are the same periodic functions of distance. Assuming the dependence $\exp(i\omega t - ikz)$, we have

$$U(z) = U(0)\exp(-ik_B z), \quad (14)$$

$$I(z) = I(0)\exp(-ik_B z).$$

For the structure of an infinite chain of periodic four-poles, from the periodicity of the structure, it follows that the displacement at period L (where N is a number of unit cells) gives

$$U(N+1) = U(N)\exp(-ik_B L) \quad (15)$$

$$I(N+1) = I(N)\exp(-ik_B L).$$

With the use of Equations (13) and (15), we have

$$\begin{pmatrix} U_N^n \\ I_N^n \end{pmatrix} = \hat{A} \begin{pmatrix} U_{N+1}^n \\ I_{N+1}^n \end{pmatrix} = \begin{bmatrix} U_{N+1}^n \exp(ik_B L) \\ I_{N+1}^n \exp(ik_B L) \end{bmatrix}. \quad (16)$$

Elements of the unimodular matrix \hat{A} , $\det \hat{A} = 1$, are expressed through elements of the matrix \hat{T}_{EC} [11]:

$$\hat{A} = \frac{1}{2} \begin{pmatrix} T_{11}^{EC} + T_{21}^{EC} + T_{12}^{EC} + T_{22}^{EC} & T_{11}^{EC} + T_{21}^{EC} - T_{12}^{EC} - T_{22}^{EC} \\ T_{11}^{EC} - T_{21}^{EC} + T_{12}^{EC} - T_{22}^{EC} & T_{11}^{EC} - T_{21}^{EC} - T_{12}^{EC} + T_{22}^{EC} \end{pmatrix}$$

$$Sp \hat{A} = Sp \hat{T}_{EC}.$$

With the use of Equations (16) and (17), we obtain

$$2 \cos k_B L = Sp \hat{T}_{EC} = T_{11}^{EC} + T_{22}^{EC}. \quad (18)$$

Finally, the Bloch equation (see, e.g., [13, 17]) has the form

$$\cos k_B L$$

$$= \cos k_1 L_1 \cos k_2 L_2 - \frac{1}{2} (r_{1,2} + r_{1,2}^{-1}) \sin k_1 L_1 \sin k_2 L_2. \quad (19)$$

Equation (19) defines the Bloch wavevector, k_B . If the absolute value of the right-hand side of Equation (19) exceeds one at some frequency, then k_B is a complex number. It thus has an imaginary part, and the field dissipates when propagating inward through the medium, which is a periodic chain of four-poles. In these conditions, the propagation of electromagnetic energy through such medium is impossible. This is the so-called forbidden band (stop band) in the spectrum of electromagnetic waves. In the case of a real k_B , we are dealing with a pass band of the medium: the electromagnetic energy freely propagates through the medium (we consider a medium without attenuation). The appearance of pass and forbidden bands in the spectrum is a characteristic feature of any periodic super-lattice. Typical spectra for an “almost infinite structure” and a “finite structure” are given in Figure 4 (we neglected the absorption). The microwave power-transmission coefficient is $D = |T_{11}|^{-2}$. Gray regions correspond to the forbidden zones of the structures. It is easy to see that the frequencies of stop bands coincided for both super-lattices, and almost do not depend on the number of cells.

3. Tamm States

Surface Tamm states are known to appear (see, e.g., [1, 3, 4]) at the boundary separating the periodic super-lattice medium (Medium 1) from Medium 2, in which the propagation of electromagnetic waves is impossible. Metals and a wire medium [4] are the most illustrative examples of such a Medium 2, but any other media with

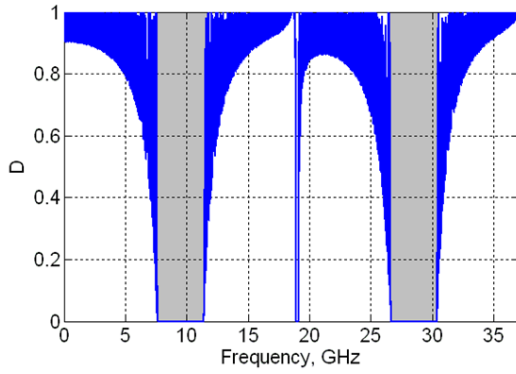


Figure 4a. The spectra for structures with various number of unit cells: The spectrum for an “almost infinite” periodic super-lattice (which means a very large number of unit cells N , ($N = 1000$))

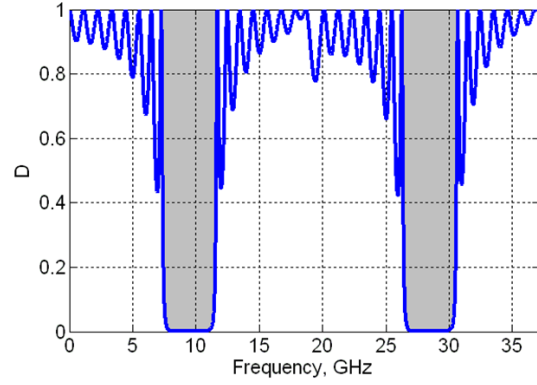


Figure 4b. The spectra for structures with various number of unit cells: The spectra for a finite structure with $N = 8$ (see Figure 5).

negative permittivity that results in strong attenuation of electromagnetic waves (Figure 1) can be used as a Medium 2. In any case, if the region of attenuation of electromagnetic waves coincides for given frequencies with the forbidden band of a periodic subsystem, the Tamm state appears, namely, the concentration of the field energy at the interface separating two media takes place. A characteristic feature of the state (as was stressed above for the two-dimensional boundary of a photonic crystal) is a homogeneous field distribution along the interface plane, between media 1 and 2. In the spectrum of the system, the Tamm state manifests itself as a sharp and narrow transmission peak, located at the frequency range where the forbidden states of both media coincide. The important case of the boundary Medium 2 can also be another periodic subsystem, the parameters of which differ from the parameters of Medium 1 (Figure 1). The only necessary condition is the coincidence of the bandgaps of both subsystems in a definite frequency range. A second subsystem (Medium 2) is a nonreflecting load line for the chain of four-poles that forms Medium 1. As in the case considered above, the Tamm states represent a sharp and narrow transmission peak in the frequency range where the forbidden bands of both media coincide. We consider this case in detail later. It should be mentioned here that due to the one-dimensionality of the considered problem, we can now speak only about an analog of the Tamm states, namely about the concentration of the electromagnetic field at the border points C between subsystems A and B.

We stress that matching of all parts of the line is an important condition in both cases, because the equality of the wave resistances (impedances) of both subsystems at the point of their contact prevents the appearance of a reflected wave in the system of four-poles.

The scheme for experimental observation of the Tamm states is presented in Figure 1. The already-mentioned condition of the equality of the impedances $Z_A = Z_B$ at the connection point is the condition of the electromagnetic waves not reflecting at this point (Z_A is the Bloch impedance of the chain of four-poles, and Z_B is the line impedance with strong attenuation or another subsystem chain, which are the

loads of the chain A). The impedance condition provides the so-called mode matching between the source and the load, i.e., provides a traveling-wave regime for the line A. Note that if the matching condition is not satisfied between the load (B) and the line (A), in general it is possible to include some matching four-pole element, which ensures fulfillment of this condition. As a result, the traveling-wave regime is restored, i.e., the line will be matched to the load. Methods for calculation of matching four-poles are described, for example, in [18].

Using Equation (16) for the unit cell in the four-poles medium, we get

$$\begin{aligned} Z_A &= \frac{U_{N+1}^n}{I_{N+1}^n} \\ &= -\frac{A_{12}}{A_{11} - \exp(ik_B L)} \quad (20) \\ &= 2 \frac{A_{12}}{(A_{11} - A_{22}) \pm \left[(A_{11} + A_{22})^2 - 4 \right]^{1/2}} \end{aligned}$$

Substituting the expressions for the matrix elements of the matrix A , we express the impedance, Z_A , in terms of known elements of the transmission matrix:

$$Z_A = 2 \frac{T_{11}^{EC} + T_{21}^{EC} - T_{12}^{EC} - T_{22}^{EC}}{(T_{21}^{EC} + T_{12}^{EC}) \pm \left[(T_{11}^{EC} + T_{22}^{EC})^2 - 4 \right]^{1/2}} \quad (21)$$

Substituting the matrix elements of the transmission matrix, Equation (10), we obtain the following expressions for the quantities entering the numerator and denominator:

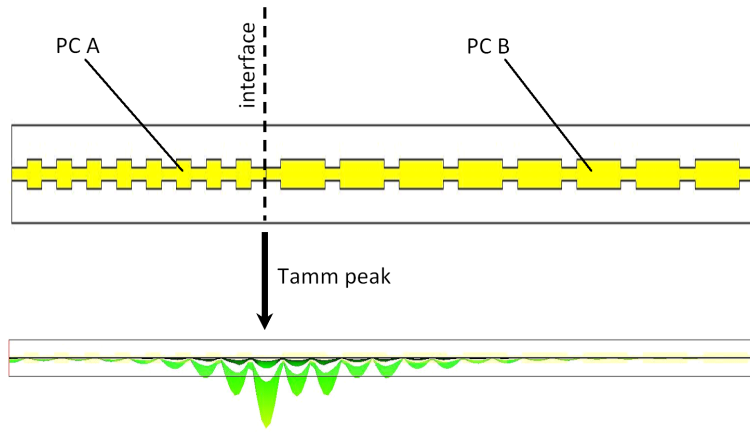


Figure 5. (top) The system used for the numerical calculations. Both super-lattices A and B consisted of eight elements. (bottom) The calculated spatial distribution of electromagnetic wave energy for the system of two subsystems.

$$T_{11}^{EC} + T_{21}^{EC} - T_{12}^{EC} - T_{22}^{EC}$$

$$= 2i(\sin k_1 L_1 \cos k_2 L_2 + r_{12} \sin k_2 L_2 \cos k_1 L_1),$$

$$T_{21} + T_{12} = (r_{12} + r_{12}^{-1}) \sin k_1 L_1 \sin k_2 L_2, \quad (22)$$

$$T_{11} + T_{22}$$

$$= 2 \cos k_1 L_1 \cos k_2 L_2 - (r_{12} + r_{12}^{-1}) \sin k_1 L_1 \sin k_2 L_2$$

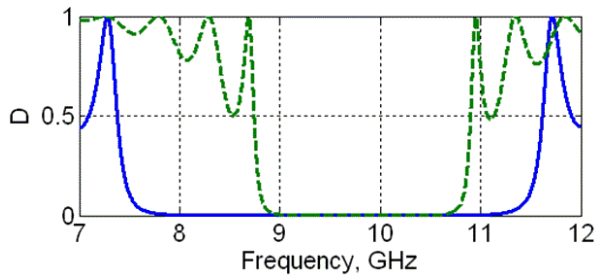


Figure 6a. The results of the numerical calculations for systems PC A and PC B: the forbidden bands for subsystems A (solid line) and B (dashed line).

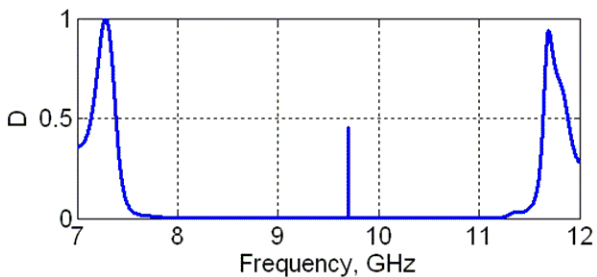


Figure 6b. The results of the numerical calculations for systems PC A and PC B: The Tamm peak at the frequency of 9.7 GHz.

Note that corresponding expressions to Equation (22) were calculated for the infinite chain.

4. Numerical Calculations

In this section, we present some results of numerical calculations carried out for the system consisting of two subsystems with various parameters of four-poles [15]. The corresponding whole system is presented in Figure 5a.

The simulation of the model structure was performed, and the details are shown in Figure 5a. The structure was a microstrip line with the following parameters. Two copper upper strips were placed on the surface of a dielectric plate (Taconic TLC-30) with $\epsilon = 3 + 0.003i$ and thickness $h = 0.5$ mm. The lower strip was a substrate strip. The upper strip was made of two periodic structures/subsystems A and B, connected in series. Each of these subsystems consisted of eight rectangular elements of equal width $D = 1.233$ mm, and their lengths were correspondingly $L_2^A = 5.0$ mm and $L_2^B = 14.2$ mm. These elements were connected with narrower rectangular elements correspondingly having equal widths $d = 3.0$ mm, and lengths $L_1^A = 5.0$ mm, mm. The characteristic impedance of such a microstrip structure equals 50 ohms at the “middle” frequency $f = 9$ GHz.

Note that in Figure 5b we can see a distribution of electromagnetic-wave energy in the system. We see the concentration of electromagnetic energy near the PC A/

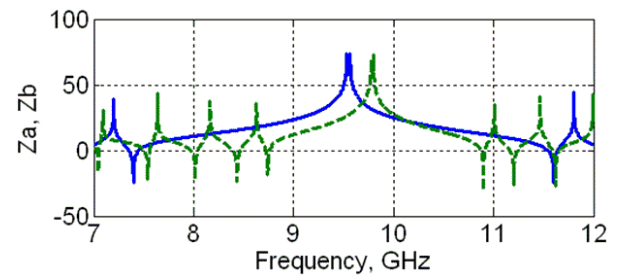


Figure 6c. The results of the numerical calculations for systems PC A and PC B: The impedances for the subsystems A (solid line) and B (dashed line).

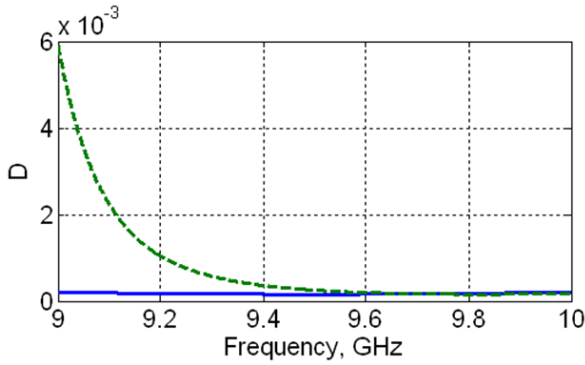


Figure 7a. The frequency dependence of the transmission coefficient in the vicinity of the Tamm peak (9 GHz to 10 GHz): The forbidden bands for each of subsystems A (solid line) and B (dashed line).

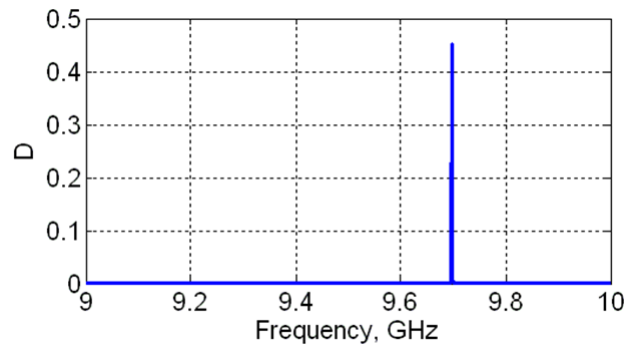


Figure 7b. The frequency dependence of the transmission coefficient in the vicinity of the Tamm peak (9 GHz to 10 GHz): The forbidden band for the joined subsystems and the position of the Tamm peak.

PC B interface. Such a concentration of energy is the analog of the Tamm state for our system.

Figure 6a presents two stop bands of two separate subsystems (PC A and PC B). The coincidence of two forbidden bands of separate subsystems takes place in the region of approximately 9 GHz to 11 GHz (the values of the transmission coefficient, D , are plotted along the y axis). The characteristic sharp increase of the microwave power-transmission coefficient, D , near a frequency of 9.7 GHz (Figure 6b) corresponds to the analog of the Tamm peak.

For the purpose of detailed analysis, we carried out numerical calculations in the vicinity of the Tamm peak, namely in the range of 9 GHz to 11 GHz. The results are presented in Figure 7.

As was stated above, the frequency position of the Tamm peak depends on the characteristics of the system. This feature of the Tamm peak is very important for various practical applications, because it enables us to control the position of the narrow transparency peak by changing the parameters of the system.

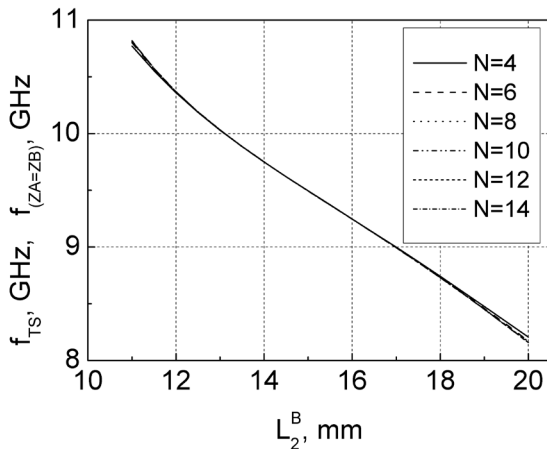


Figure 8a. The Tamm-state frequency position as a function of the value of L_2^B for various values of N : for the whole stop band, 8 GHz to 10 GHz.

In Figure 8, we present the results of numerical calculations of the dependence of the position of the Tamm peak on the magnitude L_2^B (the length of elements of the subsystem (B)). Here is also shown the dependence on L_2^B of the characteristic frequency ($f_{(ZA=ZB)}$), which is the frequency of impedance equality for both structures. Both dependencies, $f_{TS} = \varphi(L_2^B)$ (open squares) and $f_{(ZA=ZB)} = \varphi(L_2^B)$ (the solid line) coincided, and demonstrated almost linear behavior. We saw that an increase of L_2^B shifts the Tamm-state's frequency position toward the lower frequencies.

In addition, an important question is the investigation of this dependence as a function of the number of unit cells (N) in the system. According to Figure 8a, for $N = 4, 6, 8, 10, 12, 14$, all curves coincided with high accuracy. Only a small divergence took place in the vicinity of the stop band edges (Figure 8b): the divergence was higher for smaller N . This tendency is quite natural, because with the decrease of N , the system becomes more transparent, and the quality factor of the Tamm peak also decreases. The energy dissipation thus begins to play a role, and leads to the shift of the Tamm peak's frequency.

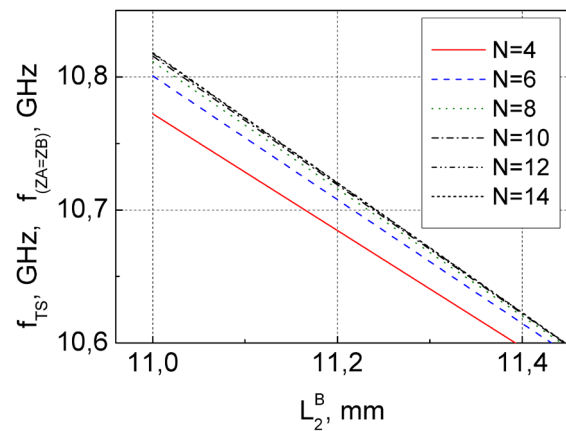


Figure 8b. The Tamm-state frequency position as a function of the value of L_2^B for various values of N : A detailed picture of the region from 10.60 GHz to 10.65 GHz on the band's edge.

5. Conclusions

1. The propagation of electromagnetic waves in systems of infinite and bounded periodical chains of four-poles was analyzed. The equation for the Bloch wave vector, determining the band structure of the infinite chain, was formulated and numerically solved.
2. A concept of the Tamm state was formulated for a periodic chain consisting of two periodic subsystems with different constitutive parameters. We revealed that this state gives rise to a concentration of electromagnetic energy in the vicinity of the interface of the two subsystems. The Tamm frequency peak corresponding to the Tamm state is located in that frequency range where the forbidden bands of the two subsystems coincide.
3. The Tamm peak's position depends on the parameters of the system, and can be changed if the parameters are changed. This feature is of great value for various practical applications of systems with Tamm states.
4. Detailed numerical calculations were carried out for the system consisting of two periodic subsystems with differing lengths of their four-pole elements. These numerical calculations verified all of the properties of the Tamm states as stated above.

6. References

1. A. P. Vinogradov, A. V. Dorofeenko, S. G. Erokhin, M. Inoue, A. A. Lisyansky, A. M. Merzlikin, A. B. Granovsky "Surface State Peculiarities in One-Dimensional Photonic Crystal Interfaces," *Phys. Rev. B*, **74**, 2006, pp. 045128.
2. I. M. Lifshitz and S. I. Pekar, "Tamm Bounded States of Electrons on the Crystal Surface and Surface Oscillations of Lattice Atoms," *Phys.-Usp.*, **56**, 4, 1955, pp. 531-568
3. A. P. Vinogradov, A. V. Dorofeenko, F. M. Merzlikin and A. A. Lisyansky, "Surface States in the Photonic Crystals," *Phys.-Usp.*, **53**, 2010, pp. 243-256.
4. S. I. Tarapov and D. P. Belozorov, "Microwaves in Dispersive Magnetic Composite Media," *Low Temperature Physics*, **38**, 7, 2012, pp. 766-792.
5. C. A. Valagiannopoulos, "Electromagnetic Propagation into Parallel-Plate Waveguide in the Presence of a Skew Metallic Surface," *Electromagnetics*, **31**, 2011, pp. 593-605.
6. C. A. Valagiannopoulos and N. K. Uzanoglu, "Green's Function of a Parallel Plate Waveguide with Multiple Abrupt Changes of Interwall Distances," *Radio Science*, **44**, 5, 2009.
7. D. A. Usanov, A. V. Skripal, A. V. Abramov, A. S. Bogolyubov, M. Y. Kulikov, D. V. Ponomarev, "Microstrip Photonic Crystals Used for Measuring Parameters of Liquids," *Technical Physics*, **55**, 8, 2010, pp. 1216-1221.
8. V. A. Neganov, *Electrodynamical Theory of Flat-Gap EHF Structures*, Saratov University, 1991 (in Russian).
9. R. A. Silin, *Periodic Waveguides*, Moscow, Phasis, 2002 (in Russian).
10. F. L. Feldshtein, L. R. Yavich, and V. P. Smirnov, *Handbook on Elements Waveguide Technology*, Moscow, Soviet Radio, 1966 (in Russian).
11. A. L. Feldshtein and L. R. Yavich, *Synthesis of 4-Pole and 8-Pole for Microwave*, Moscow, Svyaz, 1971 (in Russian).
12. L. G. Maloratsky and L. R. Yavich, *Design and Calculation Microwave Components for Strip Lines*, Moscow, Soviet Radio, 1972 (in Russian).
13. D. V. Pozar, *Microwave Engineering*, New York, John Wiley & Sons, Inc., 1998.
14. Koryu Ishii (ed.), *Handbook of Microwave Technology, Volume 1, Components and Devices*, New York, Academic Press, 1995, Chapters 2, 4.
15. R. C. Booton, *Computational Methods for Electromagnetics and Microwaves*, New York, Wiley-Interscience, 1992.
16. K. C. Gupta, R. Garg, J. Bahl, and P. Bhartia, *Microstrip Lines and Slotlines*, Norwood, MA, Artech House, 1996.
17. F. G. Bass and A. A. Bulgakov, *Kinetic and Electrodynamic Phenomena in Classical and Quantum Semiconductor Superlattices*, Nova Science Pub Inc., 1997.
18. G. D. Malushkov, *Antennas and Microwave Devices, Part 1, Transmission Lines and Microwave Devices*, Moscow, 1973 (in Russian).